IMEKO 24th TC3, 14th TC5, 6th TC16 and 5th TC22 International Conference
11 – 13 October 2022, Cavtat-Dubrovnik, Croatia

CAPACITIVE CALIBRATION CAPABILITIES IN AN EMFC BALANCE

V. Cherkasova[1], T. Fröhlich[2]

Institute for Process Measurement and Sensor Technology, Technische Universität Ilmenau
PF 10 05 65, 98684 Ilmenau, Germany
[1] valeriya.cherkasova@tu-ilmenau.de, [2] thomas.froehlich@tu-ilmenau.de

Abstract:
The article describes the possibilities of calibrating the force constant in an electromagnetic force compensation (EMFC) load cell using the electrostatic force compensation principle. The static and dynamic principles of calibration of the Kibble balance for the electrostatic force constant, as well as calibration by means of compensation of the electrostatic force by the electromagnetic force, are considered. The combination of the two compensation principles in the load cell allows the measurement of forces in the range of 20 pN to 2.2 mN and ensures traceability to national standards. The relative uncertainty in the measurement of forces of about 100 nN is estimated to be about 0.001.

Keywords: load cell; electromagnetic force compensation; electrostatic force compensation; calibration

1. INTRODUCTION

The principle of electromagnetic compensation has been widely used in load cells. They are used not only for weight measurement with the lowest uncertainty [1], but, for example, can be used for flow measurement [2] and for the calibration of cantilevers [3]. The main advantage of EMFC load cells is the linear relationship between the measured force and the Lorentz force, which leads to traceability to national standards. The electrostatic principle of compensation in load cells has not received such wide industrial acceptance, due to possible non-linearity, the need for high voltage sources and a low range of forces, but has proven itself in NIST research [4], which has achieved linear mass compensation using a concentric-cylindrical capacitor and low uncertainty measurements.

The main problem in accurate force measurement is the pre-calibration of the force constant. The most accurate calibration method is static, but it is time consuming and working only in vertical direction. Dynamic calibration methods based on the Kibble research will move the precision measurement process from a research to a commercial area.

It was decided to supplement the traceable cantilever calibration device developed at TU Ilmenau [3], which operates on the principle of electromagnetic force compensation, with electrodes in order to be able to calibrate the force constants relative to each other and expand the measurement range from 20 pN to 2.2 mN.

2. THE FUNCTIONAL PRINCIPLE OF THE DEVICE

The test stand for calibration of a cantilever with an electromagnetic and electrostatic force compensation principle is shown in Figure 1.

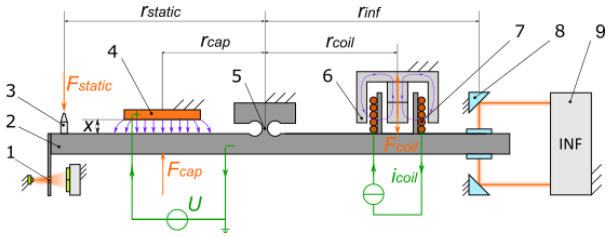

Figure 1: Test stand of the traceable cantilever calibration: (1) slit aperture; (2) beam balance; (3) push button; (4) electrode of a capacitor; (5) joint; (6) permanent magnet; (7) coil; (8) deflection mirror; (9) interferometer

The leading part of the device is the beam balance made monolithically of aluminium alloy with a swivel joint. The stiffness of the balance at the point of loading is less than 1 $N \cdot m^{-1}$, which makes it possible to calibrate small forces. When the push button (3) is subjected to a static force, the balance deflects from the zero position, the deflection is detected by one of the sensors: the slit aperture (1) or the interferometer (4). A closed loop with a controller allows to compensate the balance deflection with an electromagnetic or electrostatic force, returning it to the zero position.

The basic and most used principle of measuring the static cantilever force is based on a linear relationship between it and the compensation current of the coil in the permanent magnet field attached to the weight beam:

$$F_{\text{static}} = B \cdot l \cdot i_{\text{coil}} \cdot \frac{r_{\text{coil}}}{r_{\text{static}}}, \quad (1)$$

where $B \cdot l$ is the electromagnetic force constant, depending on the magnetic-flux density and the length of the coil; r_{coil} is the radius from the joint to the coil; and r_{static} is the radius from the joint to the push button.

Another principle is to compensate the static force by the electrostatic force. Since the balance is entirely made of aluminium alloy, we can consider it as a cathode and one of the plate electrodes as an anode. Given the distance and air between them, one can imagine that their combination is a structure of the plate-shaped capacitor. The static force is related to the square of the voltage applied to the capacitor:

$$F_{\text{static}} = \frac{1}{2} \cdot \frac{\mathrm{d}C}{\mathrm{d}x} \cdot U^2 \cdot \frac{r_{\text{cap}}}{r_{\text{static}}}, \quad (2)$$

where $\frac{1}{2} \cdot \frac{\mathrm{d}C}{\mathrm{d}x}$ is electrostatic force constant, capacitive gradient and r_{cap} is the radius from the joint to the centre of the capacitor.

Despite the non-linearity of the compensation force, the main advantages of using electrostatic compensation are the absence of mechanical influence of wires on measurements and the possibility of measuring small forces in pN.

3. STATIC AND DYNAMIC ELECTROSTATIC KIBBLE BALANCE CALIBRATION METHODS

A schematic representation of the electrode used in the study is shown in Figure 2.

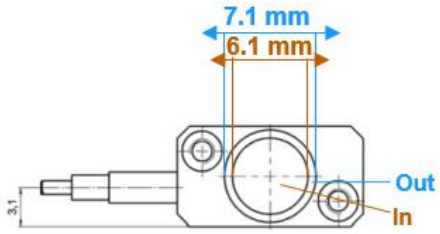

Figure 2: Anode PI D015 [5]

The inner conductor of the coaxial cable is connected to the inner circle, the braided shield to the outer.

The cathode – balance is connected to ground: all aluminium parts of the device, including the aluminium platform height 40 cm and the stainless steel vacuum chamber. Figure 3 shows the device in the vacuum chamber with protective covers.

The initial distance between the anode and the cathode is less than 50 µm. The anode area is 29.225 mm^2. Since the distance between the electrodes is much less than the root of the area, edge effects are not taken into account when calculating the capacitance.

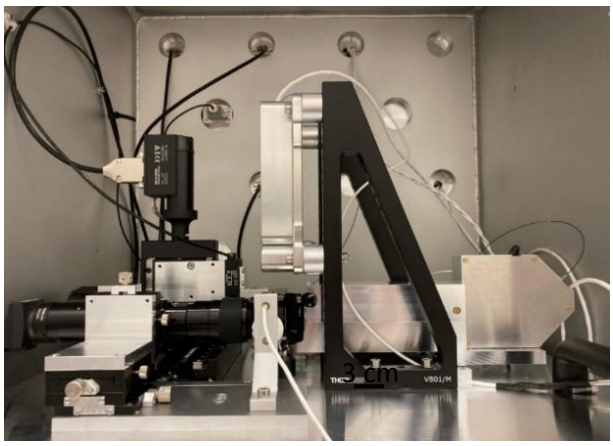

Figure 3: The traceable cantilever calibration device

3.1 Static Calibration with a Hioki Impedance Analyser

A classic option for capacitive gradient calibration is static calibration, force mode in the Kibble balance. The method consists in changing the distance between the plates of the capacitor at a given distance and, accordingly, measuring the capacitance with impedance analyser or capacitance to digital converter at each step:

$$K_{\text{es}} = \frac{1}{2} \cdot \frac{\mathrm{d}C}{\mathrm{d}x} = -\frac{1}{2} \cdot \frac{\varepsilon_0 \cdot \varepsilon_{\text{r}} \cdot A}{(x_0 + x_{\text{d}})^2}, \quad (3)$$

where ε_0 is the absolute dielectric permittivity (vacuum), ε_{r} is the relative permittivity, A is the effective cross section of the capacitor, x_0 is the initial distance between the two electrodes, and x_{d} is the change of the distance in z-direction.

The Hioki Impedance Measurement Handbook [6] states that Hioki devices cannot measure impedance on grounded samples (Figure 4). Current leakage may occur when measuring a grounded sample.

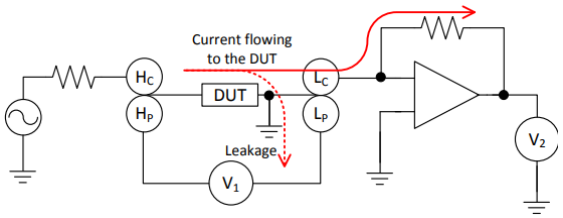

Figure 4: Current path for a grounded DUT

The study was carried out with the Hioki IM3570 analyser. Figure 5 shows options for connecting the analyser to the electrodes and the current path.

The anode position is fixed. The position of the cathode is changed in equal steps by controlling the coil current. The distance is read by the interferometer. The distance between the electrodes is calculated based on the ratio of the levels from the CAD model. The measured change in the capacitance depending on the distance between the electrodes is shown in Figure 6.

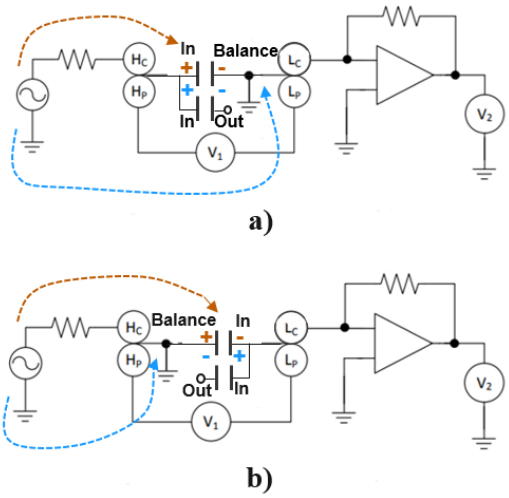

Figure 5: Current path for a grounded DUT: a) current leakage, b) no current leakage

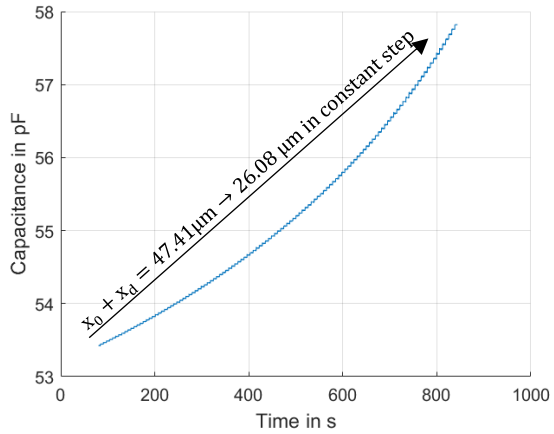

Figure 6: Measured capacitance by an impedance analyser

Figure 7 shows the dependence of the electrostatic factor on the distance between the electrodes.

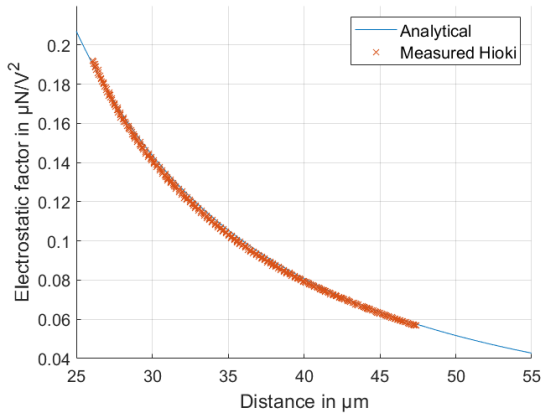

Figure 7: Electrostatic factor calculated from Hioki data

The deviation between the analytically obtained force constant and the one calculated on the basis of the measured data depends on dissipative losses during measurement, uncertainties in estimating the level of the electrode position and uncompensated additional capacitances from the conductors.

From equation (3) and Figure 7 it is possible to see the advantages of the electrostatic compensation: the value of the electrostatic force constant can be increased by means of decreasing the initial distance between the balance and the plate or increasing the effective cross-sectional area of the plate. With a decrease in the initial position between the electrodes from 40 µm to 26 µm, the electrostatic factor increases by a factor of 2.5.

3.2 Static Calibration with Wire Weight

Another option for static calibration of the electrostatic force constant is to use an E_1 class wire weight or E_0 with PTB calibration certificate [7]. A wire weight of 1 mg with a tolerance of 1.5 µg from Häfner Gewichte GmbH was used in the study. Compensating for a known weight load allows the calibration constant to be calculated as follows:

$$\begin{aligned} F_{\text{static}} &= m \cdot g \\ F_{\text{es}} &= K_{\text{es}} \cdot (U_2^2 - U_1^2 + 2V_{\text{s}}(U_2 - U_1)) \\ K_{\text{es}} &= \frac{m \cdot g}{(U_2^2 - U_1^2 + 2V_{\text{s}}(U_2 - U_1))} \cdot \frac{r_{\text{static}}}{r_{\text{cap}}}, \end{aligned} \tag{4}$$

where U_1 is the voltage on capacitor before loading weight, U_2 is the compensated voltage on capacitor after loading weight, and V_{s} the surface voltage [4].

The appearance of a surface potential can be caused by a variable work function on a polycrystalline metal surface with an electrostatically inhomogeneous surface. But the contact surface potential cannot be measured, as each measuring device has its own surface potential, and measurements are also affected by adsorption on the electrodes and their contamination.

The value of the surface voltage can be found from the difference in the required compensating force when using positive and negative voltage for the same weight.

Figure 8 shows a graph of the positive compensation voltage when the balance is loaded with the weight of 1 mg.

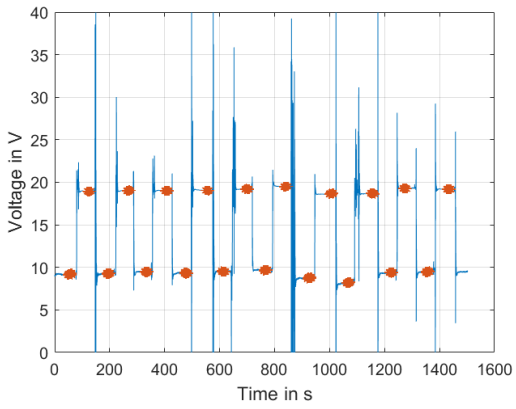

Figure 8: Blue – measured positive compensated voltage, brown – subsequently averaged compensation voltage values for analysis

Disturbances on the graph are caused by manual placement of the weight on the balance. The difference in compensation voltage levels is also caused by fluctuations in the control signal. Automation of the loading process due to a piezo drive based on a single point will significantly reduce the measurement uncertainty and is planned for the future. Comparison of the electrostatic factor with the analytical calculation is shown in Figure 9.

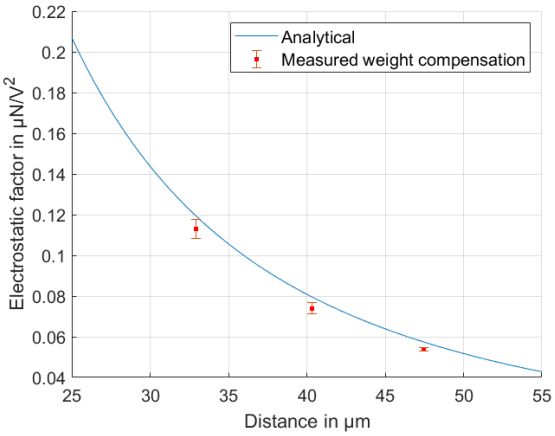

Figure 9: Electrostatic factor calculated from weight compensation force

As can be seen from the graph, the measured characteristic curve correlates qualitatively with the analytical calculation, the relative deviation is less than 4.3 %. Reducing mechanical disturbances, taking into account the temperature coefficient and optimal voltage control will reduce the resulting difference.

3.3 Dynamic Calibration

The velocity mode in the Kibble balance can be used to dynamically calibrate the electrostatic constant. It is necessary that the balance is set in motion, for this purpose a piezoelectric element with an elastic metal sheet or the voice coil actuator can be used. Due to the relative motion, a current is induced, which can be measured through a resistor. A constant operating voltage is applied to both electrodes of the capacitor, the induced current is the time derivative of the charge. The sinusoidal movement is detected by the interferometer, so the electrode velocity can be derived from the time derivative of the position.

$$i_{\mathrm{ind}}(t) = \frac{\mathrm{d}Q}{\mathrm{d}t} = \frac{\mathrm{d}(C \cdot U_{\mathrm{a}})}{\mathrm{d}t} = U_{\mathrm{a}} \cdot \frac{\mathrm{d}C}{\mathrm{d}t}$$

$$i_{\mathrm{ind}}(t) = -U_{\mathrm{a}} \cdot \dot{x_{\mathrm{d}}} \cdot \frac{\varepsilon_0 \cdot \varepsilon_{\mathrm{r}} \cdot A}{(x_0 + x_{\mathrm{d}})^2} \qquad (5)$$

$$K_{\mathrm{es}} = -\frac{1}{2} \cdot \frac{\varepsilon_0 \cdot \varepsilon_{\mathrm{r}} \cdot A}{(x_0 + x_{\mathrm{d}})^2} = \frac{i_{\mathrm{ind}}(t)}{2 \cdot U_{\mathrm{a}} \cdot \dot{x_{\mathrm{d}}}},$$

where U_{a} is the constant actuation voltage, $i_{\mathrm{ind}}(t)$ is the induced current, measured with shunt resistor, and $\dot{x_{\mathrm{d}}}$ is the analytically-calculated electrode velocity from the measured distance.

The results of measuring the induced current when a sinusoidal signal is applied to the coil are shown in Figure 10. The resulting electrostatic factor in comparison with the analytical calculation is defined in Figure 11. On the basis of the measured sinusoidal movement of the balance, the analytically induced current (brown) was calculated, on the basis of which the electrostatic factor was determined, which qualitatively corresponds to the analytical calculations for static calibration. Represented in yellow, the electrostatic factor derived from the induced current measurements is currently very noisy; by using a precision resistor and signal filtering it will be possible to accurately estimate the deviation.

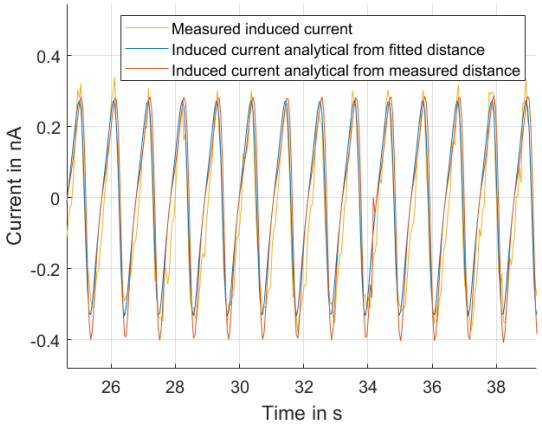

Figure 10: Comparison of the induced current

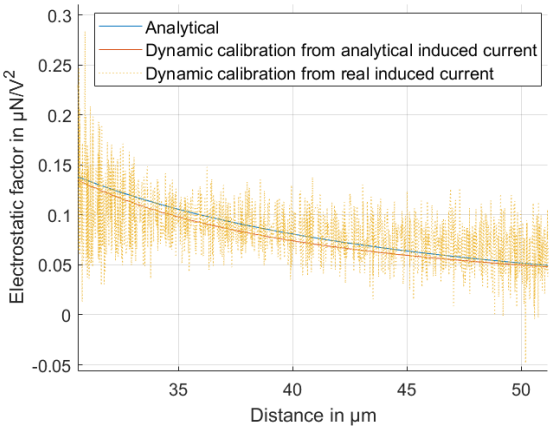

Figure 11: Electrostatic factor calculated from dynamic calibration

3.4 Static Calibration with Electromagnetic Force

By combining the electromagnetic and electrostatic principles of the Kibble calibration in one device, it is possible to calibrate an unknown force based on a known one. For example, the electromagnetic force constant can be calibrated by a static method prior to the experiment, so the electrostatic calibration factor based on the electromagnetic force compensation will be:

$$K_{\mathrm{es}} = \frac{1}{2} \cdot \frac{\mathrm{d}C}{\mathrm{d}x} = B \cdot l \cdot \frac{i_{\mathrm{coil}}}{U^2} \cdot \frac{r_{\mathrm{coil}}}{r_{\mathrm{cap}}}. \quad (6)$$

To obtain the gradient of the electrostatic factor, measurements are made at different distances between the balance and the electrode. The balance is controlled by the coil current at reference positions. As in section 3.2, the calculation is affected by surface voltage. Thus, in order to obtain reliable results, the compensation current of the coil is measured when the capacitor is influenced to both positive and negative potential. Figure 12 shows the compensating force as a function of the applied voltage.

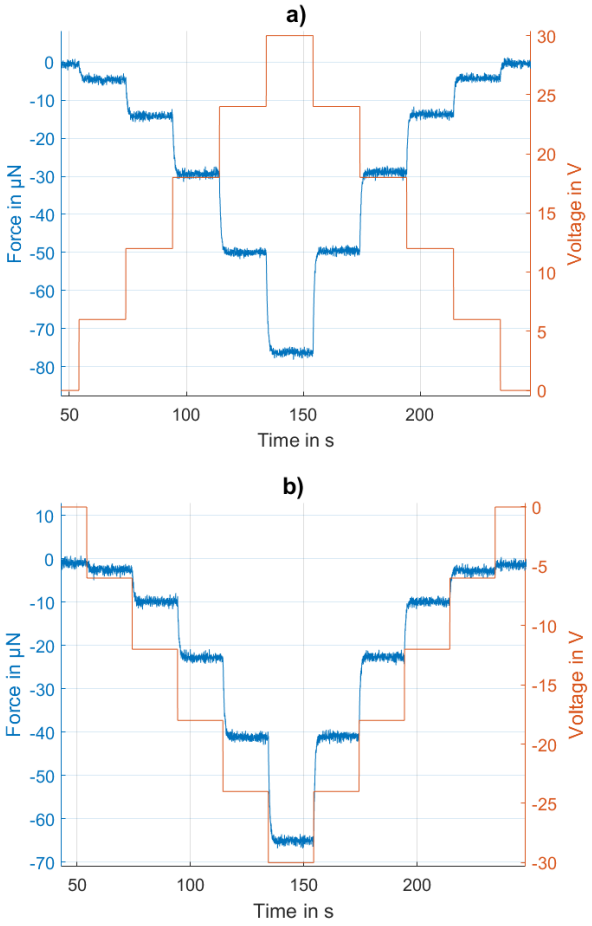

Figure 12: a) Compensating electromagnetic force when voltage is stepped on the capacitor from 0 V to 30 V in steps of 5 V, b) compensating electromagnetic force when voltage is stepped on the capacitor from 0 V to -30 V in steps of -5 V

The maximum compensation force differs by more than 10 µN when applied to the capacitor from the source |30| V. Accordingly, the effect of surface voltage cannot be attributed to uncertainties and must be taken into account in every measurement. Comparison of the analytically calculated electrostatic factor and the factor obtained from the electromagnetic compensation force is shown in Figure 13.

The discrepancy between the measured electrostatic coefficient and the analytically calculated one was 1 %.

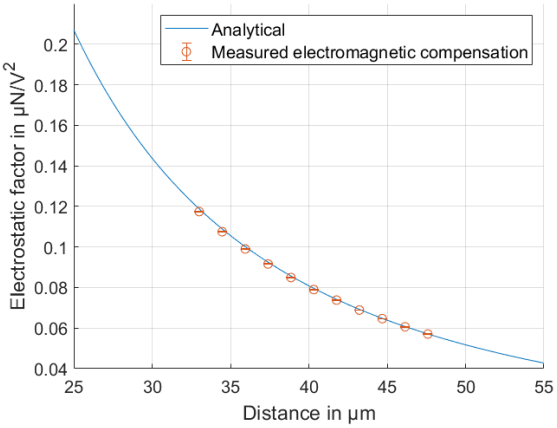

Figure 13: Electrostatic factor calculated from electromagnetic compensation force

4. OUTLOOK

The biggest disadvantage of using electrostatic forces is square non-linearity. In a further study, two identical electrodes will be used to achieve a linear relationship in the differential electrostatic force actuator. A schematic description is shown in Figure 14.

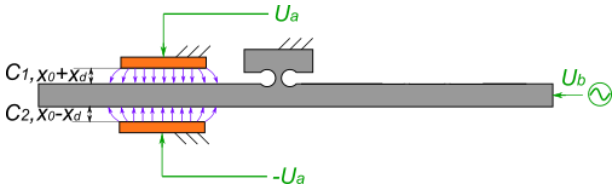

Figure 14: Schematic of the electrostatic force actuator

Since the electrodes have the same geometry and are located symmetrically with respect to the balance, the capacitance gradients of both capacitors are equal in value and opposite in direction at the equilibrium position. The following are the force output equations for a differential electrostatic force actuator:

$$\frac{\mathrm{d}C_1}{\mathrm{d}x} = -\frac{\mathrm{d}C_2}{\mathrm{d}x}$$

$$C_1 = \frac{\varepsilon_0 \cdot \varepsilon_{\mathrm{r}} \cdot A}{x_0 + x_{\mathrm{d}}}, C_2 = \frac{\varepsilon_0 \cdot \varepsilon_{\mathrm{r}} \cdot A}{x_0 - x_{\mathrm{d}}}$$

$$C_2 - C_1 = \frac{\varepsilon_0 \cdot \varepsilon_{\mathrm{r}} \cdot A \cdot 2 \cdot x_{\mathrm{d}}}{{x_0}^2 - {x_{\mathrm{d}}}^2}, \quad (7)$$

for ${x_{\mathrm{d}}}^2 \ll {x_0}^2$:

$$C_2 - C_1 = \frac{\varepsilon_0 \cdot \varepsilon_{\mathrm{r}} \cdot A \cdot 2 \cdot x_{\mathrm{d}}}{{x_0}^2}$$

$$F_{\mathrm{es}} = \frac{1}{2} \cdot \frac{\mathrm{d}C_1}{\mathrm{d}x} [(U_{\mathrm{a}} - U_{\mathrm{b}})^2 - (-U_{\mathrm{a}} - U_{\mathrm{b}})^2]$$

$$F_{\mathrm{es}} = 2 \cdot \frac{\mathrm{d}C_1}{\mathrm{d}x} \cdot U_{\mathrm{a}} \cdot U_{\mathrm{b}} \,,$$

where U_{a} is the applied voltage and U_{b} is the bias voltage.

Figure 15 shows the scale of the possible measurement range based on the technical capabilities of the system.

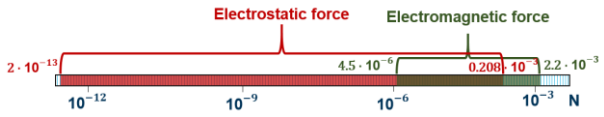

Figure 15: Measurement range

Our results suggest that forces of around 100 nN can be realised with an estimated relative uncertainty of less than 0.001. A detailed uncertainty analysis according to GUM is planned for the near future.

5. SUMMARY

Combining the electromagnetic and electrostatic compensation principle increases the possibility of calibrating force constants and expands the area of force measurement from pN to mN. A linear relationship between the measured force and the electrostatic force can be achieved by adjusting the differential electrostatic field using an additional electrode identical to the one already installed.

The authors gratefully acknowledge the colleagues in force measuring and weighing technology: N. Rogge, S. Vasilyan, M. Pabst, and the support by the Deutsche Forschungsgemeinschaft (DFG) in the scope of the Research Training Group "Tip- and Laserbased 3D-Nanofabrication in extended macroscopic working areas" (GRK 2182) at Technische Universität Ilmenau, Germany.

6. REFERENCES

[1] C. Rothleitner, N. Rogge, S. Lin, S. Vasilyan, D. Knopf, F. Härtig, T. Fröhlich, “Planck-Balance 1 (PB1) - a table-top Kibble balance for masses from 1 mg to 1 kg - current status”, Acta IMEKO, vol. 9, no. 5, pp. 47-52, 2020.
DOI: 10.21014/acta_imeko.v9i5.937

[2] N. Yan, S. Vasilyan, M. Kühnel, T. Fröhlich, “Investigation to the tilt sensitivity of the Lorentz force velocimetry system for the flow rate measurement of low conducting fluids”, in Proc. IMEKO, 2017.

[3] O. Dannberg, T. Fröhlich, “Stiffness calibration of AFM cantilevers”, tm-Technisches Messen, vol. 88, no. s1, pp. 3-7, 2021.
DOI: 10.1515/teme-2021-0046

[4] G. A. Shaw, J. Stirling, J. A. Kramar, A. Moses, P. Abbott, R. Steiner, A. Koffman, J. R. Pratt, Z. J. Kubarych, “Milligram mass metrology using an electrostatic force balance”, Metrologia, vol. 53, no. 5, p. A86, 2016.
DOI: 10.1088/0026-1394/53/5/A86

[5] Physik Instrumente (PI) GmbH & Co. KG, “Capacitive Sensors, D-015, D-050, D-100”, Datasheet, 2015. Online [Accessed 20221216]: https://usermanual.wiki/Physik-Instrumente/PIDatasheetD015D050D1002015012 0pdf.371679873/view

[6] Hioki E.E. Corporation, “Impedance Measurement Handbook”, 2018.

[7] International Organization of Legal Metrology. OIML R 111-1, “Weights of classes E_1, E_2, F_1, F_2, M_1, M_{1-2}, M_2, M_{2-3} and M_3 – Part 1: Metrological and technical requirements”, 2004.

[8] S. Vasilyan, N. Rogge, C. Rothleitner, S. Lin, I. Poroskun, D. Knopf, T. Fröhlich, “The progress in development of the Planck-Balance 2 (PB2): A tabletop Kibble balance for the mass calibration of E_2 class weights”, tm-Technisches Messen, vol. 88, no. 12, pp. 731-756, 2021.
DOI: 10.1515/teme-2021-0101

[9] J. C. Lotters, W. Olthuis, P. H. Veltink, P. Bergveld, “A sensitive differential capacitance to voltage converter for sensor applications”, IEEE Transactions on Instrumentation and Measurement, vol. 48, no. 1, pp. 89-96, 1999.
DOI: 10.1109/19.755066

[10] S. Lin, C. Rothleitner, N. Rogge, T. Fröhlich, “Influences on amplitude estimation using three-parameter sine fitting algorithm in the velocity mode of the Planck-Balance”, Acta IMEKO, vol. 9, no. 3, pp. 40-46, 2020.
DOI: 10.21014/acta_imeko.v9i3.781